ASIAN JOURNAL OF CIVIL ENGINEERING (BHRC) VOL. 18, NO. 6(2017)
PAGES 977-992

THREE-DIMENSIONAL NONLINEAR SEISMIC RESPONSE OF OUED FODDA CONCRETE GRAVITY DAM CONSIDERING CONTACT ELEMENTS AT DAM-RESERVOIR INTERACTION INTERFACE

D. Ouzandja[1*], B. Tiliouine[2], M. Belharizi[3] and M. Kadri[4]
[1]Laboratory of Materials and Mechanics of Structures (LMMS), University of Msila, Algeria
[2]Civil Engineering Department, Ecole Nationale Polytechnique, 10 Avenue H. Badi, 16200 Algiers, Algeria
[3]37 Impasse Armand, 92160 Antony, France,
[4]Civil Engineering Department, Faculty of Technology, University of Boumerdes, Algeria

Received: 18 February 2017; **Accepted:** 12 May 2017

ABSTRACT

This paper aims to present the three-dimensional nonlinear seismic response of concrete gravity dams considering contact elements at dam-reservoir interaction interface. Dam-reservoir contact interface is modeled with three-dimensional surface-to-surface contact elements based on the Coulomb's friction. A numerical investigation of the effect of hydrodynamic interaction and sliding of the water along the dam-reservoir interface is performed. The maximum horizontal displacements and principal stresses in the different sections of the dam are presented as well as seismic behavior of dam is examined in empty and full reservoir cases. Besides, the damage placements in the concrete dam are evaluated.

Keywords: Concrete gravity dam; dynamic dam-reservoir interaction; Lagrangian approach; contact elements; nonlinear seismic response; finite element method.

1. INTRODUCTION

The building of dams in seismic zone constitutes a permanent potential danger to the surrounding population, and a major concern for governments. Accordingly, it is necessary to study precisely the dynamic behavior of dams in order to evaluate their performance under the different predicted earthquakes.

There are several phenomenons affecting the dynamic behavior of concrete dams to

*E-mail address of the corresponding author: dj_ouzandja@yahoo.com (D. Ouzandja)

seismic excitations. These are generally the dam-foundation and dam-reservoir interaction. Many researches were carried out on the dam-foundation interaction problem by a lot of researchers [1-9].

In the literature, two approaches may be used to model the dam-reservoir interaction phenomenon, the coupling method and contact elements. For the first approach, the main objective of the coupling approach is to hold equal the displacements between two reciprocal nodes in the normal direction to the interface. But, the dam body and reservoir fluid haven't the same material properties, their interaction should be modeled by using different nodes at connection interface. In the second approach, the contact interface between the dam and the water reservoir is modeled by interface and contact elements which provide the friction contact.

In recent years, the dynamic contact problems became nonlinear and nonsmooth [10-12], and a part of the discipline of contact mechanics [13-15], which has allowed to treat effectively the different contact phenomenons in engineering field and its applications. Several researches were based on the use of interface elements in order to study seismic response of concrete gravity dams including dam-foundation rock interaction [16-21]. Arabshahi and Lotfi [22] studied the seismic response of gravity dams considering interface elements between the dam base and the foundation rock to model sliding and opening along the dam-foundation contact interface. Kartal [23] presented the earthquake response of roller-compacted concrete dams considering dam-foundation-reservoir interaction using three-dimensional finite element model. The structural connections in dam-foundation-reservoir interaction interface are modeled by using contact elements. The effect of variation of friction coefficient based on the contact elements at dam-foundation interface on the seismic response of concrete gravity dams was investigated by Ouzandja and Tiliouine [24].

Besides, contact elements have a wide field of use to present the interaction phenomenon between different media, in particular fluid-structure interaction. However, the use of these elements to describe dam-reservoir interaction remains limited in published literature compared to approach when the coupling elements are employed.

The seismic response of Oued Fodda concrete gravity dam including fluid-structure interaction was performed by various stydies [25-29] using the coupling technic. In the present paper, the main objective is to present the three-dimensional nonlinear seismic response of Oued Fodda concrete gravity dam considering contact elements at dam-reservoir interaction interface using the finite element method. For illustrative purposes, a numerical investigation of the effect of hydrodynamic interaction and sliding of the water along the dam-reservoir interface is carried out. The hydrodynamic pressure of reservoir water is modeled using three-dimensional fluid finite elements based on Lagrangian approach. The Drucker-Prager model [30] is employed in the nonlinear analysis for concrete of dam body. The horizontal and vertical components of 1967 Koyna earthquake are utilized in analyses. Dam-reservoir contact interface is modeled with three-dimensional surface-to-surface contact elements based on the Coulomb's friction, which can provide friction contact. The different numerical analyses are performed using ANSYS software [31].

2. CONTACT MECHANICS

Many contact problems involve deformations of the bodies that are in contact. To illustrate the contact concept, consider two solids in contact on parts of their border (Fig.1). That is to say $\{n\}$ the outbound norm on the surface of the one of solids in contact and $\{u\}$ the vector displacement between two solids. Then $g = \langle u \rangle . \{n\}$ is project displacement on this norm. From the data of the stress of Cauchy, one defines the pressure $p = \langle n \rangle . [\sigma] . \{n\}$ and the shearing stress tangential $\{\tau\} = [\sigma] . \{n\} - p . \{n\}$ as being exerted by one of surfaces on the other [32].

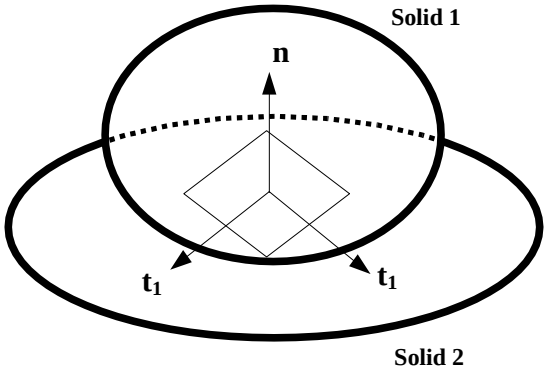

Figure 1. Contact mechanism of solid bodies [32]

The shear force has as a direction in the contact zone a vector $\{t\}$ located in the tangent plane ($\{t_1\}$, $\{t_2\}$) indicated on the Fig.1. The equation (1) defines the shearing stress τ exerted by the solid 2 on the solid 1 per unit of contact surface.

$$\{\tau\} = [\sigma] . \{n\} - (\langle n \rangle . [\sigma] . \{n\}) . \{n\} = \tau . \{t\} \text{ with } \tau = \|\{\tau\}\| \tag{1}$$

We introduce two variables defining the contact: signed distance between the two surfaces or "gap" g and contact pressure P. The mathematical condition for non-penetration is stated as $g \geq 0$ which precludes the penetration of solid 1 into solid 2. Contact takes place when g is equal to zero. In this case, the contact pressure p in the contact interface must be non-zero. If the bodies come into contact, $g = 0$ and $P < 0$. If there is a gap between the bodies, $g > 0$ and $P = 0$. This leads to the statements

$$g \geq 0; \;\; P \leq 0; \;\; P\, g = 0 \tag{2}$$

which are known as Hertz-Signorini-Moreau conditions [15].

2.1 Friction model

In the basic Coulomb friction model, two contacting surfaces can carry shear stresses up to a certain magnitude across their interface before they start sliding relative to each other. This state is known as sticking. The Coulomb friction model below [31] shown in Fig. 2 defines

an equivalent shear stress τ, at which sliding on the surface begins as a fraction of the contact pressure p. This stress is:

$$\tau = \mu p + c \tag{3}$$

where μ is the friction coefficient and c specifies the contact cohesion. Once the shear stress is exceeded, the two surfaces will slide relative to each other. This state is known as sliding. The maximum contact friction stress can be introduced so that, regardless of the magnitude of normal contact pressure, sliding will occur if the friction stress reaches this value. At the contact interface, the connection behavior is divided into two kinematic states:

If the shear stress is less than the maximum friction stress, no relative displacement takes place in the contact region. This is named sticking which can be described by the condition:

$$\tau_{max} < \mu p + c \tag{4}$$

Once the shear stress becomes higher than the maximum friction stress, the contact bodies move relative to each other. This is named sliding which can be formulated by:

$$\tau_{max} \geq \mu p + c \tag{5}$$

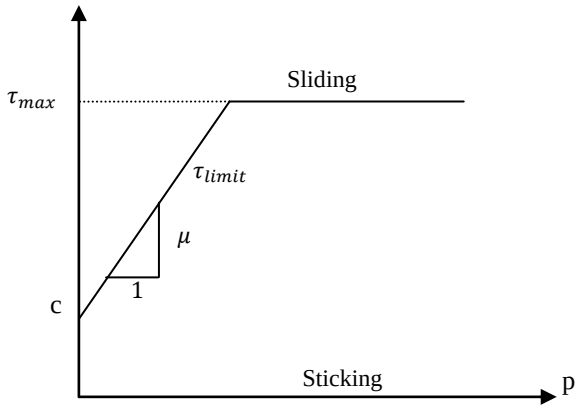

Figure 2. Coulomb friction model [31]

3. NUMERICAL MODEL

3.1. Material properties

Chosen dam is sited on Oued Fodda River and approximately 20 km of Oued Fodda City, Chlef, Algeria (Fig. 3). The reservoir is mainly used for irrigation purposes. The capacity of the dam is 125.5 hm^3. The maximum height and base width of the dam are 101 m and 67.5 m, respectively. The dam crest is 190 m in length and 5 m wide and the maximum height of the reservoir water is considered as 101 m. The reservoir width is 300 m. The transverse and longitudinal sections of the dam-reservoir coupled system are shown in Fig. 4.

Figure 3. Oued Fodda concrete gravity dam

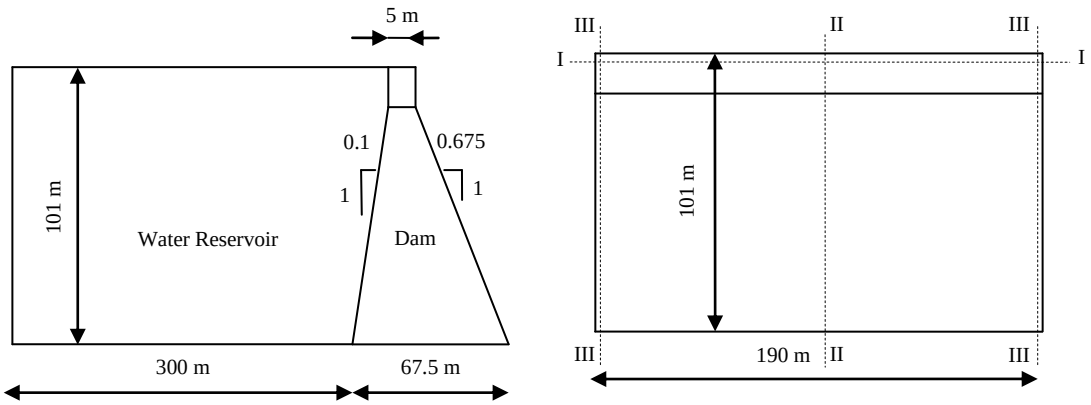

(a) Transverse section and dimensions (b) Longitudinal section and dimensions

Figure 4. Sections and dimensions of the Oued Fodda concrete gravity dam

The material properties for both the dam and its water reservoir are given in Table 1. According to the Drucker-Prager model [30], the cohesion and the angle of internal friction of the dam body are assumed as to be 2.50 Mpa and 35°, respectively. In addition, the tensile strength and the compressive strength of the concrete of the dam are 1.6 MPa and 20 MPa, respectively.

Table 1: Material properties of Oued Fodda concrete gravity dam and its water reservoir

Material	Material properties		
	Modulus of elasticity (MPa)	Poisson's ratio	Mass density (kg/m^3)
Dam (concrete)	24600	0.20	2640
Reservoir water	2070	-	1000

3.2 Three-dimensional finite element model of dam-reservoir system

The formulation of the dam-reservoir interaction system is represented using the Lagrangian approach [33-36], which considers that the fluid is assumed linear-elastic, incompressible, inviscid, and irrotational [37].

The dam-resevoir interaction system is investigated using the three-dimensional finite element model shown in Fig. 5. A three-dimensional finite element model with 3400 solid finite elements (Solid45) is used to model Oued Fodda dam. Besides, a three-dimensional finite element model with 4760 fluid finite elements (Fluid80) is used to model the reservoir water. The fluid element (Fluid80) is used to model fluids contained within vessels having no net flow rate. The fluid element is particularly well suited for calculating hydrostatic pressures and fluid-solid interactions [31]. In addition, 340 contact-target element pairs are employed to model dam-reservoir interaction interface.

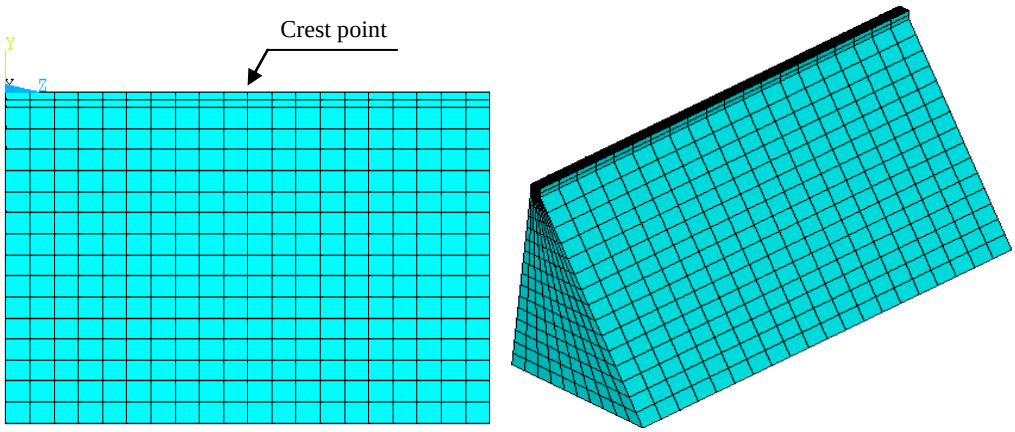

(a) Upstream face of dam (b) Dam in empty reservoir case

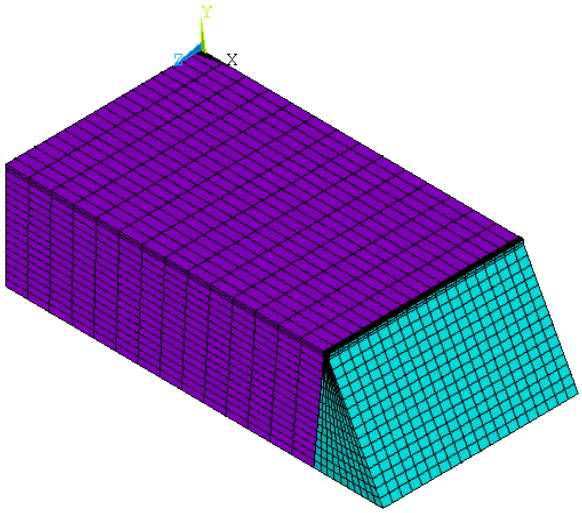

c) Dam in full reservoir case

Figure 5. Three-dimensional finite element model of dam-reservoir system

3.3 Modeling of dam-reservoir contact interface

The seismic response of a concrete dam depends upon its contact interaction with the water reservoir. This interaction interface between the dam and reservoir of water is modeled by using contact elements. These elements can present the contact and sliding of the water along the dam-reservoir interface and provide the friction response by the properties of normal and tangential shear stiffness at contact interface. In this study, three-dimensional contact elements which represent the friction contact are established between the surfaces of volumes for three-dimensional system. Surface-to-sutface contact elements generated by ANSYS software [31] are chosen. These contact elements use a target surface (Targe170) and a contact surface (Conta174) to form a contact pair. In addition, "no separation" contact model is employed in this purpose which allows the sliding of contact surfaces. The Coulomb friction and contact friction stress are available in these elements.

4. RESULTS AND DISCUSSION

4.1 Nonlinear seismic response of Oued Fodda dam

This study investigates the three-dimensional nonlinear seismic response of Oued Fodda concrete gravity dam considering contact elements at dam-reservoir interaction interface. For this purpose, the horizontal and vertical components of 1967 Koyna earthquake are utilized in analyses (Fig. 6). The horizontal component is applied along the river axis. The Drucker-Prager model [30] is used in the nonlinear analysis for concrete of the dam body. All numerical analyses are carried out using ANSYS [31]. The maximum horizontal displacements and principal stresses in upstream face along the different sections of the dam are presented for both empty and full reservoir cases.

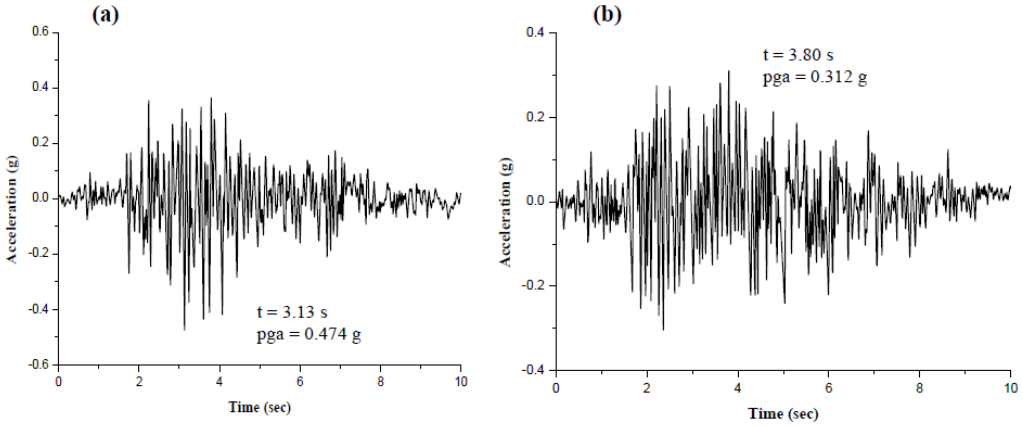

Figure 6. Acceleration records of 1967 Koyna earthqake: (a): Horizontal component and (b): Vertical component

4.1.1 Horizontal displacements

The maximum horizontal displacements in upstream face of the dam along the I-I and II-II sections are respectively presented in Figs. 7-8.

4.1.1.1 I-I Section

The horizontal displacements of the dam in I-I section are presented in Fig. 7 for both empty and full reservoir cases. According to numerical analyses, the hydrodynamic pressure of reservoir water increases the horizontal displacements in upstream face along the dam crest. As seen in Fig. 7, the maximum displacements occur at middle of the dam and dam crest for both cases. However, the maximum horizontal displacements obtained from full reservoir case are higher than ones obtained from empty reservoir case.

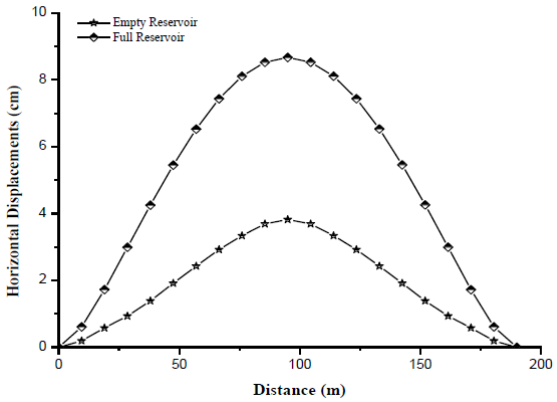

Figure 7. Maximum horizontal displacements in upstream face along the dam crest in I-I section

4.1.1.2 II-II section

The variation of horizontal displacements of the dam along its height in II-II section is shown in Fig. 8 for both empty and full reservoir cases. Numerical analyses illustrate that the horizontal displacements increase in upstream face along the dam central axis by the effect of hydrodynamic pressure of the reservoir water. It is observed that the maximum horizontal displacements appear at the dam crest point in full reservoir case.

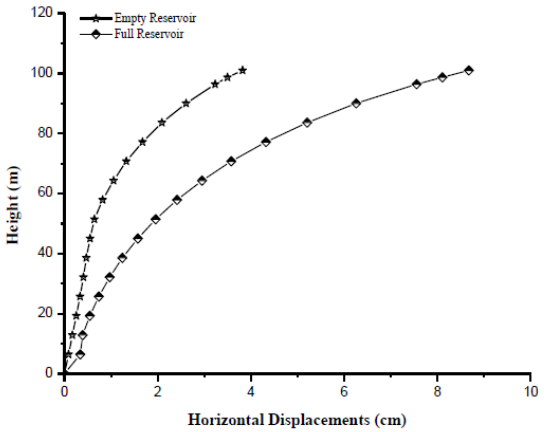

Figure 8. Maximum horizontal displacements in upstream face along the dam central axis in II-II section

Fig. 9 represents the maximum horizontal displacement contours of the dam under hydrodynamic pressure. It is clear that the maximum displacements occur at the middle region of the dam crest.

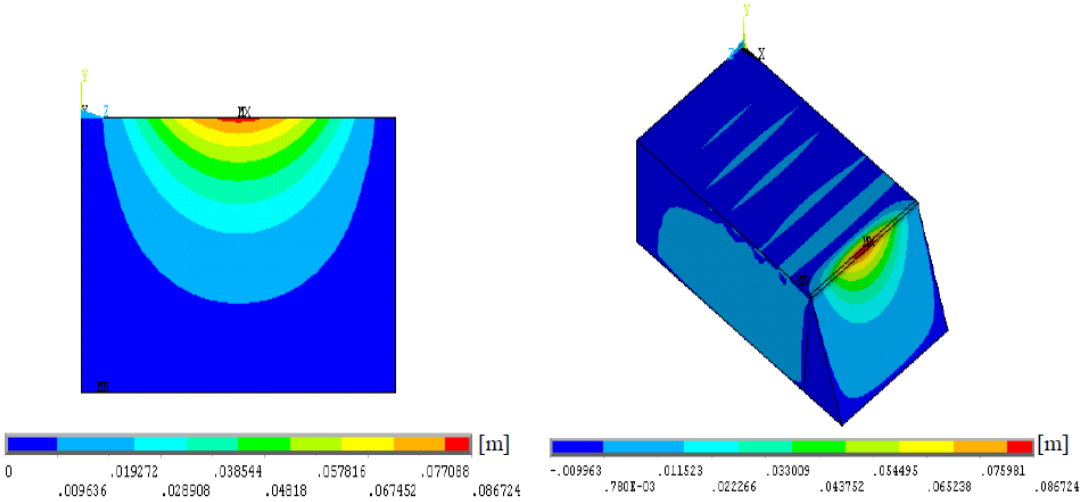

(a) Upstream face of dam (b) Dam-reservoir coupled system

Figure 9. Maximum horizontal displacement contours of the dam under hydrodynamic pressure.

Fig. 10 shows the time history of horizontal displacement at the dam crest (crest point) in upstream face for empty and full reservoir cases. The maximum horizontal displacements at this point are equal to 3.82 cm and 8.67 cm, respectively, for empty and full reservoir cases. Therefore, an increase of 127 % is observed between the results of the two cases. It is obvious that the horizontal displacements obtained from full reservoir case are higher than ones obtained from empty reservoir case due to the effect of hydrostatic and hydrodynamic pressure of the reservoir water.

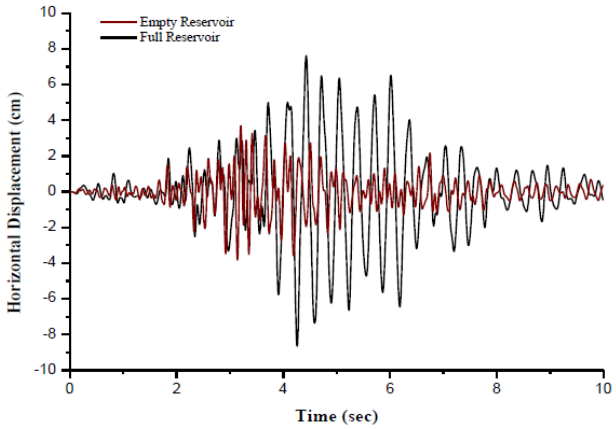

Figure 10. Time history of horizontal displacement at the dam crest in upstream face for empty and full resservoir cases

4.1.2 Principal stresses

The maximum principal stresses in upstream face of the dam along the I-I, II-II and III-III sections are respectively shown in Figs. 11-13.

4.1.2.1. I-I section

The maximum principal stresses into the dam along the I-I section are presented in Fig. 11 for both empty and full reservoir cases. Accoding to numerical analyses, the hydrodynamic pressure of reservoir water increases principal tensile and compressive stresses in upstream face along the dam crest. As seen in Fig. 11, the maximum principal stresses occur especially at the crest and extremity regions of the dam along the I-I section in full reservoir case. The maximum principal tensile stresses have a decreasing trend for the distance between 0 and 30 m, but they have an increasing trend for the distance between 30 and 95 m. Besides, the maximum principal compressive stresses have a decreasing trend fot the distance between 0 and 20 m, but they have an increasing trend for the distance between 20 m and 95 m.

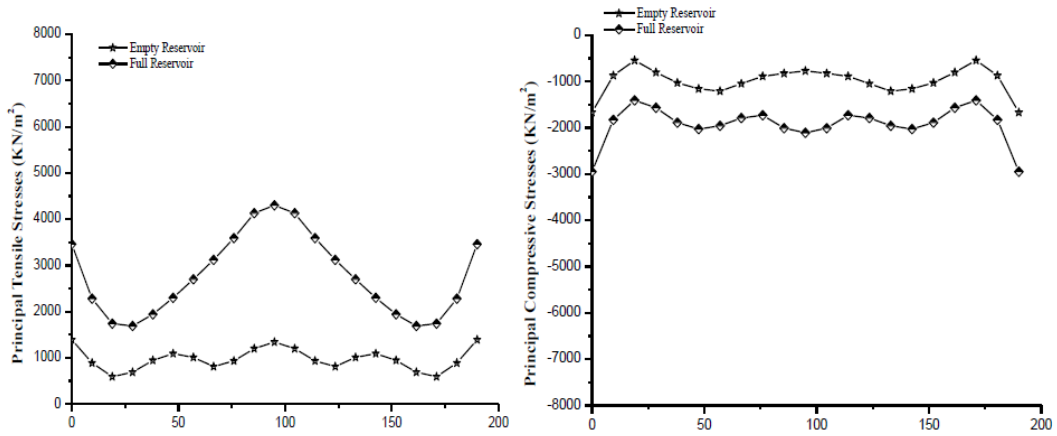

(a) Maximum principal tensile stresses (b) Maximum principal compressive stresses

Figure 11. Maximum principal stresses along the dam crest in I-I section

4.1.2.2 II-II section

The variation of maximum principal stresses into the dam along its height in II-II section is shown in Fig. 12 for both empty and full reservoir cases. Numerical analyses indicate that hydrodynamic pressure of reservoir water increase the maximum principal stresses in upstream face along the dam central axis. It is observed that the maximum principal compressive stresses occur at bottom of dam in full reservoir case. However, the principal compressive stresses become greater from a height of 60 m in empty reservoir case. In addition to this, the maximum principal tensile stresses appear at the dam crest in full reservoir case.

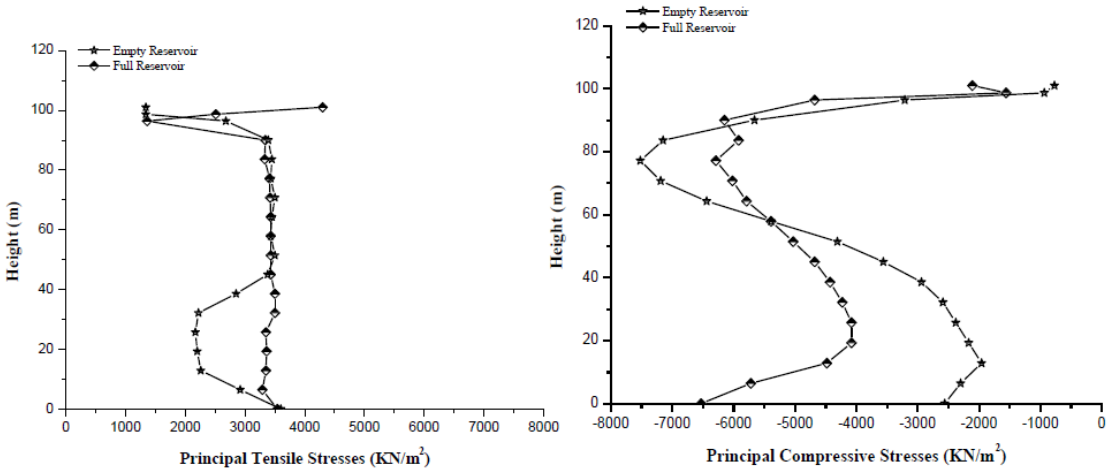

(a) Maximum principal tensile stresses (b) Maximum principal compressive stresses

Figure 12. Maximum principal stresses along the dam central axis in II-II section

4.1.2.3 III-III section

The maximum principal stresses into the dam along the III-III section are presented in Fig. 13 for both empty and full reservoir cases. Numerical analyses show that the maximum principal stresses along the extremity axis of dam are obtained in full reservoir case. As seen in Fig, 13, the maximum principal compressive stresses occur by effect of hydrodynamic pressure at the height of 80 m from the base of the dam. In addition, the maximum principal tensile stresses under hydrodynamic pressure appear greater over 35 m of the dam.

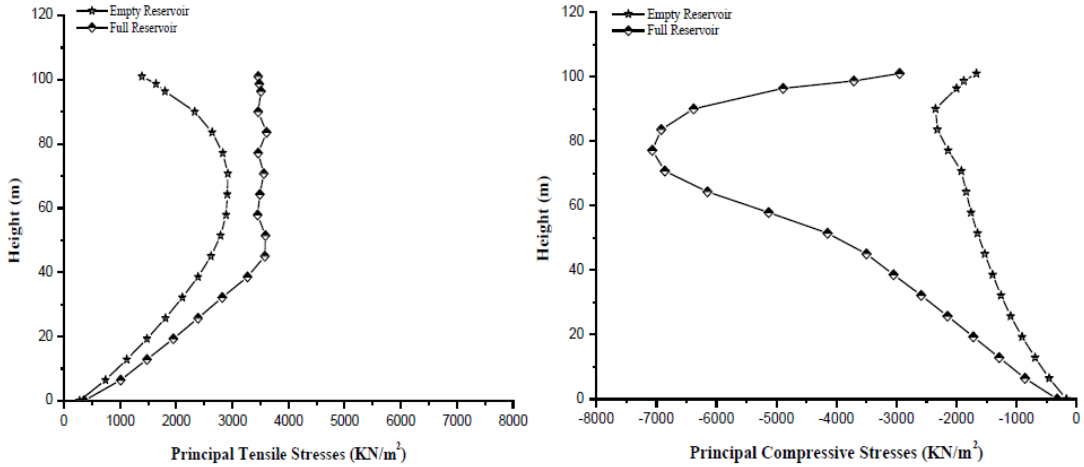

(a) Maximum principal tensile stresses (b) Maximum principal compressive stresses

Figure 3. Maximum principal stresses along the dam extremety axis in III-III section

Fig. 14 represents the maximum principal tensile and compressive stresses contours of the dam under hydrodynamic pressure. It is observed that the maximum principal stresses

occur at the middle region of the dam crest, upper and lower parts along the symmetry central axis and upper extremity regions of the dam.

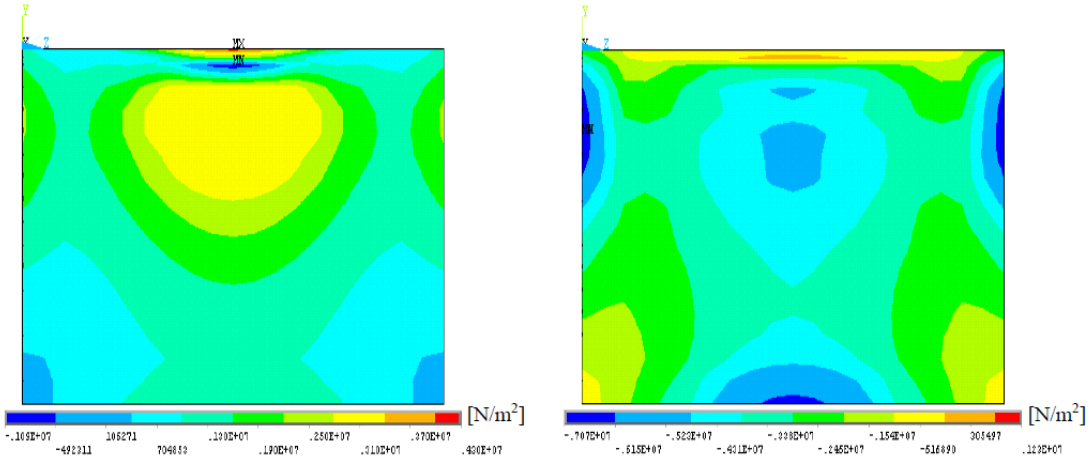

(a) Maximum principal tensile stress contours (b) Maximum principal compressive stress contours

Figure 14. Maximum principal stresses contours in upstream face of dam under hydrodynamic pressure

Fig. 15 illustrates the time history of principal stresses at the dam crest in upstream face for empty and full reservoir cases. The maximum principal tensile and compressive stresses increase from 1.34 E3 kN/m^2 and -7.71 E2 kN/m^2 in empty reservoir case to 4.30 E3 kN/m^2 and -2.11 E3 kN/m^2 in full reservoir case. Therefore, for full reservoir model, an increase of 221 % and 174 % respectively, in the magnitude of maximum principal tensile and compressive stresses is noticed. It is obvious that the principal tensile and compressive stresses are greatly higher under the effect of hydrodynamic pressure.

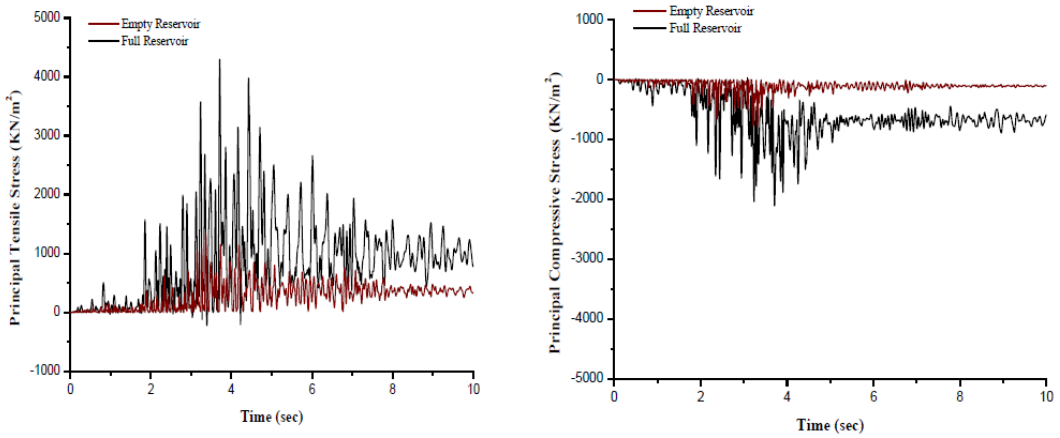

(a) Principal tensile stresseses (b) Principal compressive stresses

Figure 15. Time history of principal stresses at the dam crest in upstream face for empty and full resservoir cases

The maximum principal tensile strain contours of the dam under hydrodynamic pressure are presented in Fig. 16. It is seen that these strain contours occur where the maximum principal tensile stresses occurred. Fig. 17 illustrates the time history of maximum principal tensile strains at the dam crest in upstream face for full reservoir case. Howevere, the obtained values of maximum strains into the dam are lower than the admissible strains of the concrete [38-39].

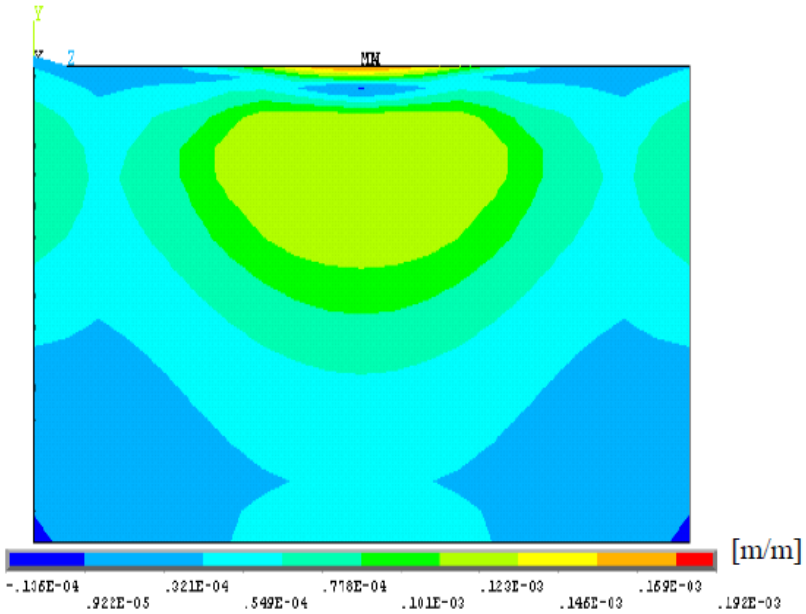

Figure 16. Maximum principal tensile strain contours in upstream face of the dam under hydrodynamic pressure

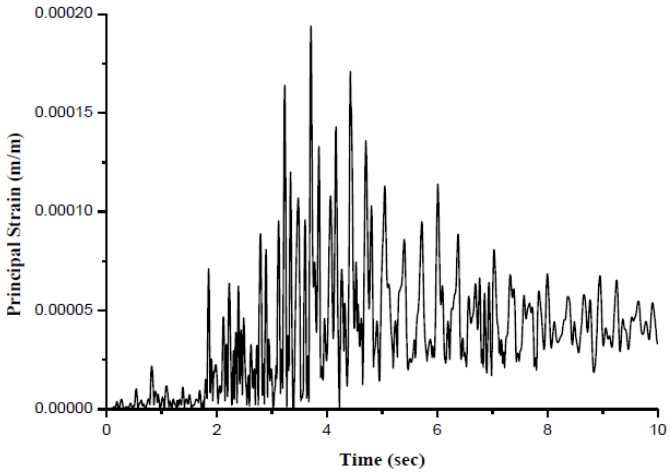

Figure 17. Time history of maximum principal tensile strains at the dam crest in upstream face for full reservoir case

5. CONCLUSIONS

This study presents the three-dimensional nonlinear seismic response of Oued Fodda concrete gravity dam considering contact elements at dam-reservoir interaction interface. For this purpose, a numerical investigation of the effect of hydrodynamic interaction and sliding of the water along the dam-reservoir interface is performed. The Drucker-Prager model [30] is used in the nonlinear analysis for concrete of dam body. The hydrodynamic pressure of reservoir fluid is modeled using fluid finite elements based on Lagrangian approach.

According to different numerical results performed in this study, we can draw the following conclusions:

1. The hydrodynamic pressure of the reservoir water increases the horizontal displacements of the dam. The maximum horizontal displacements occur at the middle region of dam crest.
2. The hydrodynamic pressure of the reservoir water increases the principal stresses in the dam body. The maximum principal tensile stresses have a decreasing trend for the distance between 0 and 30 m, but they have an increasing trend for the distance between 30 and 95 m.
3. The maximum principal tensile stresses occur at the middle region of the dam crest, upper and lower parts along the symmetry central axis and upper extremity regions of the dam. Hence it is expected to appear cracks in these parts causing damage in the dam.
4. The hydrostatic and hydrodynamic pressure of the reservoir water should be taken into account in the numerical analyses to evaluate the critical response of the dam.
5. The generated strains occurred in the acceptable intervals for the concrete employed in the dam body.

The dam-reservoir interaction problem is a complex phenomenon. It depends upon the material pairing of the bodies constituting the contact region between the dam and water reservoir (contact interface). This description is adapted to the use of contact elements which can identify the parts to be analyzed for the interaction. Therefore, the contact elements should be taken into account in the modeling of the dam-reservoir interaction phenomenon to achieve more reliable results, due to the capacity of these elements to present the contact and sliding of the water along the dam-reservoir interface.

REFERENCES

1. Chopra Ak, Chakrabarti P. Earthquake analysis of concrete gravity dams including dam-water-foundation rock interaction, *Earthquake Engineering & Structural Dynamics*, No. 4, **9**(1981) 363-83.
2. Leger P, Boughoufalah M. Earthquake input mechanisms for time domain analysis of damfoundation systems, *Engineering Structures*, No. 1, **11**(1989) 37-46.
3. Bayraktar A, Hancer E, Akkse M. Influence of base-rock characteristics on the stochastic dynamic response of dam-reservoir-foundation systems, *Engineering Structures*, No. 10, **27**(2005) 1498-508.

4. Saleh S, Madabhushi SPG. Response of concrete dams on rigid and soil foundations under earthquake loading, *Earthquake Tsunami*, No. 3, **4**(2010) 251-68.
5. Lebon G, Saouma V, Uchita Y. 3D rock-dam seismic interaction, *Dam Engineering*, No. 2, **21**(2010) 101-30.
6. Saouma V, Miura F, Lebon G, Yagome Y. A simplified 3D model for soil-structure interaction with radiation damping and free field input, *Bulletin of Earthquake Engineering*, No. 5, **9**(2011) 1387-402.
7. Burman A, Nayak P, Agrawal P, Maity D. Coupled gravity dam-foundation analysis using a simplified direct method of soil-structure interaction, *Soil Dynamic Earthquake Engineering*, No. 1, **34**(2012) 62-68.
8. Hariri-Ardebili MA. Impact of foundation nonlinearity on the crack propagation of high concrete dams, *Soil Mechanics and Foundation Engineering*, No. 2, **51**(2014) 72-82.
9. Ouzandja D, Benkechida F, Ouzandja T. Study of dynamic soil-structure interaction of concrete gravity dams, *Proceeding of the Second European Conference on Earthquake Engineering and Seismology* (2ECEES), Istanbul, Turkey, 2014.
10. Belytschko T, Liu WK, Moran B. *Nonlinear Finite Elements for Continua and Structures*, John Wiley & Sons, Ltd, Chichester, 2000.
11. Laursen TA. *Computational Contact and Impact Mechanics: Fundamentals of Modeling Interfacial Phenomena in Nonlinear Finite Element Analysis*, Springer, Berlin, 2002.
12. Wriggers P. *Computational Contact Mechanics*, John Wiley & Sons, Ltd, New York, 2002.
13. Kikuchi N, Oden JT. Contact problems in Elasticity: A Study of Variational Inequalities and Finite Element Methods, SIAM, Philadelphia, 1988.
14. Zhong ZH. Finite element procedures for contact-impact problems, Oxford University Press Inc, New York, 1993.
15. Wriggers P. *Computational Contact Mechanics*, 2nd eddition, Wiley/Springer, Berlin, Heidelberg, 2006.
16. Leger P, M Katsouli M. Seismic stability of concrete gravity dams, *Earthquake Engineering & Structural Dynamics*, No. 6, **18**(1989) 889-902.
17. Chopra AK, Zhang L. Earthquake-induced base sliding of concrete gravity dams, *Journal of Structure Engineering*, No. 12, **117**(1991) 3698-719.
18. Danay A, Adeghe LN. Seismic induced slip of concrete gravity dams, *Journal of Structure Engineering, ASCE*, No.1, **119**(1993) 108-29.
19. Chavez JW, Fenves GL. Earthquake analysis of concrete gravity dams including base sliding, *Earthquake Engineering & Structural Dynamics*, No. 5, **24**(1995) 673-86.
20. Chavez JW, Fenves GL. Earthquake analysis of concrete gravity dams including base sliding, *Journal of Structure Engineering, ASCE*, No. 5, **121**(1995) 865-75.
21. Viladkar MN, Al-Assady AMS. Nonlinear analysis of pine flat dam including base sliding and separation, *Proceeding of the Fifteenth World Conference on Earthquake Engineering (15 WCEE)*, Lisbon, Portugal, 2012.
22. Arabshahi H, Lotfi V. Earthquake response of concrete gravity dams including dam-foundation interface nonlinearities, *Engineering Structures*, No. 11, **30**(2008) 3065-73.
23. Kartal ME. Three-dimensional earthquake analysis of roller compacted concrete dams, *Natural Hazards and Earthquake System Sciences*, **12**(2012) 2369-88.

24. Ouzandja D, Tiliouine B. Effects of dam-foundation contact conditions on Seismic Performance of Concrete Gravity Dams, *Arabian Journal for Science and Engineering*, No. 11, **40**(2015) 3047-56.
25. Tiliouine B, Seghir A. Influence de l'interaction fluide-structure sur le comportement sismique du barrage de Oued Fodda (Nord-Ouest Algérien), *Proceeding of the Conference CAM97*, Damas, Syrie, 1997.
26. Tiliouine B, Seghir A. Fluid-structure models for dynamic studies of dam-water systems, *Proceeding of the Eleventh European Conference on Earthquake Engineering*, Paris, France, 1998.
27. Tiliouine B, Seghir A. A numerical model for time domain analysis of dams including fluid-structure interaction, *Proceeding of the Fourth International Conference on Computer Structures Technology CST98*, Edinburg, Scotland, 1998.
28. Seghir A, Tahakourt A. Analyse dynamique des systèmes barrage-réservoir avec couplage éléments finis-éléments infinis, *Proceeding du 7ème Colloque de l'Association Française de Génie Parasismique*, Paris, France, 2007.
29. Seghir A, Tahakourt A, Bonnet G. Coupling FEM and symmetric BEM for dynamic interaction of dam-reservoir systems, *Engineering Analysis with Boundary Elements*, No. 10, **33**(2009) 1201-10.
30. Drucker DC, Prager W. Soil mechanics and plastic analysis of limit design, *Quarterly of Applied Mathematics*, No. 2, **10**(1952) 157-65.
31. ANSYS. Theory user's manual, Swanson Analysis Systems Inc, Houston, PA, USA, 2012.
32. Abbas M. Discrete formulation of the contact-friction, Reference Documentation of Code_Aster N° R5.03.50; 1013.
33. Wilson EL, Khalvati M. Finite elements for the dynamic analysis of fluid-solid systems, *International Journal for Numerical Methods in Engineering*, No. 11, **19**(1983) 1657-68.
34. Nomura T, Thomas JRH. An arbitrary Lagrangian-Eulerian finite element method for interaction of fluid and a rigid body, *Computer Methods in Applied Mechanics and Engineering*, No.1, **95**(1992) 115-38.
35. Calayır Y. Dynamic analysis of concrete gravity dams using the Eulerian and the Lagrangian approaches, Dissertation, Karadeniz Technical University, Terkey, 1994.
36. Van Loon R, Anderson PD, Van de Vosse FN, Sherwin SJ. Comparison of various fluid-structure interaction methods for deformable bodies, *Computer and Structures*, Nos. 11-14, **85**(2007) 833-43.
37. Young-Surck K, Chung-Bang Y. A spurious free four-node displacement fluid element for fluid-structure interaction analysis, *Engineering Structures*, No. 8, **19**(1997) 665-78.
38. Swaddiwudhipong S, Lu HR, Wee TH. Direct tension test and tensile strain capacity of concrete at early age, *Cement and Concrete Research*, No. 12, **33**(2003) 2077-84.
39. Sutherland B. Experimental and analytical analysis of the stress-strain diagram of frp-confined concrete with different loading rates, M.S. Thesis, Department of Civil Engineering, Kansas State University, USA, 2006.